

MOX–Report No. 50/2013

**A two-level method for Mimetic Finite Difference  
discretizations of elliptic problems**

ANTONIETTI, P.F.; VERANI, M.; ZIKATANOV, L.

MOX, Dipartimento di Matematica “F. Brioschi”  
Politecnico di Milano, Via Bonardi 9 - 20133 Milano (Italy)

mox@mate.polimi.it

<http://mox.polimi.it>



# A two-level method for Mimetic Finite Difference discretizations of elliptic problems

Paola F. Antonietti<sup>b</sup>, Marco Verani<sup>b</sup>, and Ludmil Zikatanov<sup>‡</sup>

October 14, 2013

<sup>b</sup> MOX, Dipartimento di Matematica, Politecnico di Milano  
Piazza Leonardo da Vinci 32, I-20133 Milano, Italy  
E-mail: [paola.antonietti@polimi.it](mailto:paola.antonietti@polimi.it)

<sup>b</sup> MOX, Dipartimento di Matematica, Politecnico di Milano  
Piazza Leonardo da Vinci 32, I-20133 Milano, Italy  
E-mail: [marco.verani@polimi.it](mailto:marco.verani@polimi.it)

<sup>‡</sup> Department of Mathematics, Penn State University  
University Park, PA 16802, USA. E-mail: [ludmil@psu.edu](mailto:ludmil@psu.edu)

## Abstract

We propose and analyze a two-level method for mimetic finite difference approximations of second order elliptic boundary value problems. We prove that the two-level algorithm is uniformly convergent, *i.e.*, the number of iterations needed to achieve convergence is uniformly bounded independently of the characteristic size of the underlying partition. We also show that the resulting scheme provides a uniform preconditioner with respect to the number of degrees of freedom. Numerical results that validate the theory are also presented.

## 1 Introduction

Thanks to its great flexibility in dealing with very general meshes and its capability of preserving the fundamental properties of the underlying physical model, the mimetic finite difference (MFD) method has been successfully employed, in approximately the last ten years, to solve a wide range of problems. Mimetic methods for the discretization of diffusion problems in mixed form are presented in [23, 26, 24, 25]. The primal form of the MFD method is introduced and analyzed in [21, 13]. Convection–diffusion problems are considered in [29, 9], while the problem of modeling flows in porous media is addressed [44]. Mimetic discretizations of linear elasticity and the Stokes equations are presented in [8] and [10, 12, 11], respectively. MFD methods

have been used in the solution of Reissner-Mindlin plate equations [18], and electromagnetic [20, 43] equations. Numerical techniques to improve further the capabilities of MFD discretizations such that *a posteriori* error estimators [7, 15, 1] and post-processing techniques [28] have been also developed. The application of the MFD method to nonlinear problems (variational inequalities and quasilinear elliptic equations) and constrained control problems governed by linear elliptic PDEs is even more recent, see [3] for a review. More precisely, in [4, 2] a MFD approximation of the obstacle problem, a paradigmatic example of variational inequality, is considered. The question whether the MFD method is well suited for the approximation of optimal control problems governed by linear elliptic equations and quasilinear elliptic equations is addressed in [6] and [5], respectively. Recently, in [16], the mimetic approach has been recast as the *virtual element method* (VEM), cf. also [27, 17]. Nevertheless, efficient solvers for the (linear) systems of equations arising from MFD discretizations are still being developed. The main difficulty in the development of optimal multilevel solution methods relies on the construction of consistent coarsening procedures which are non-trivial on grids formed by more general polyhedra. We refer to [42, 46, 41] for recent works on constructing coarse spaces with approximation properties in the framework of the agglomeration multigrid method.

The aim of this paper is to develop an efficient two-level method for the solution of the linear systems of equations arising from MFD discretizations of a second order elliptic boundary value problem. We prove that a two-level algorithm that rely on the construction of suitable prolongation operators between a hierarchy of meshes is uniformly convergent with respect to the characteristic size of the underlying partition. We also show that the resulting scheme provides uniform preconditioner, *i.e.*, the number of Preconditioned Conjugate Gradient (PCG) iterations needed to achieve convergence up to a (user-defined) tolerance is uniformly bounded independently of the number of degrees of freedom. An important observation is that for unstructured grids (such as the MFD grids) a two-level (and multilevel) method is optimal if the number of nonzeros in the coarse grid matrices is under control. This is important for practical applications and one of the main features of the method proposed here is that we modify the coarse grid operator so that the number of nonzeros in the corresponding coarse grid matrix is under control. This in turn complicates the analysis of the preconditioner, since we need to account for the fact that the bilinear form on the coarse grid is no longer a restriction of the fine grid bilinear form.

The layout of the paper is as follows. In Section 2 we introduce the model problem and its mimetic finite difference discretization. The solvability of the discrete problem is discussed also in this section and further, a Poincaré-type inequality is proved in Section A. Our two-level method is described and analyzed in Section 3. Finally, in Section 4 we present numerical results

to validate the theoretical estimates of the previous sections and to test the practical performance of our algorithms.

## 2 Model problem and its mimetic discretization

Let  $\Omega$  be an open, bounded Lipschitz polygon in  $\mathbb{R}^2$ . Using the standard notation for the Sobolev spaces, we consider the following variational problem: Find  $u \in H_0^1(\Omega)$  such that

$$\int_{\Omega} \kappa(\mathbf{x}) \nabla u \cdot \nabla v \, d\mathbf{x} = \int_{\Omega} f v \, d\mathbf{x}, \quad \text{for all } v \in H_0^1(\Omega). \quad (1)$$

Here,  $f \in L^2(\Omega)$  and we assume that the function  $\kappa(\mathbf{x})$  is a piece-wise constant function, bounded and strictly positive, namely, there exist  $\kappa_{\star} > 0$ , and  $\kappa^{\star} > 0$  such that  $\kappa_{\star} \leq \kappa(\mathbf{x}) \leq \kappa^{\star}$ .

We now briefly review the mimetic discretization method for problem (1) presented in [22] and extended to arbitrary polynomial order in [14]. Roughly speaking, the mimetic method is a discretization on a polygonal partition of  $\Omega$  which satisfies appropriate consistency conditions. In the following, to avoid the proliferation of constants, by  $\lesssim$  we denote an upper bound that holds up to an unspecified positive constant. Moreover, in the sequel, we will denote by  $(\cdot, \cdot)$  the Euclidean scalar product in  $\ell^2(\mathbb{R}^n)$ , *i.e.*,  $(u, v) = \sum_{i=1}^n u_i v_i$  for any  $u = (u_1, u_2, \dots, u_n), v = (v_1, v_2, \dots, v_n) \in \mathbb{R}^n$ .

### 2.1 Domain partitioning

We first introduce the notation pertinent to the specifics of the mimetic method under consideration. We partition  $\Omega$  as union of connected, closed polygonal subdomains with non-empty interior. We denote this partition with  $\Omega_h$ , that is, we have  $\Omega = \cup_{E \in \Omega_h} E$  with  $E$  being closed and with nonempty interior. We assume that this partition is conforming, *i.e.*, the intersection of two different elements  $E_1$  and  $E_2$  is either empty or is a union of lower dimensional polygons. More precisely, the intersection of two elements  $E_1$  and  $E_2$  is union of vertices or union of edges. One notable difference with the conforming finite element mesh, is that a  $T$ -junctions are now allowed in the mesh. Indeed, adding a mesh point at the junction corresponds to splitting single edge into two edges.

For each polygon  $E \in \Omega_h$ ,  $|E|$  denotes its area,  $h_E$  denotes its diameter and  $h = \max_{E \in \Omega_h} h_E$  is the characteristic size of the partition  $\Omega_h$ . The set of vertices and edges of the partition is denoted by  $\mathcal{N}_h$  and  $\mathcal{E}_h$ , respectively. We further have the set of interior vertices and edges  $\mathcal{N}_h^i$  and  $\mathcal{E}_h^i$ , and the set of boundary vertexes and edges by  $\mathcal{N}_h^{\partial}$  and  $\mathcal{E}_h^{\partial}$ . The vertices and edges of

a particular element  $E$  are denoted by  $\mathcal{N}_h^E$  and  $\mathcal{E}_h^E$ , respectively. A generic vertex will be denoted by  $\mathbf{v}$ , and a generic edge by  $e$ . For the length of an edge we will use the symbol  $h_e$ . A fixed orientation is also set for the mesh  $\Omega_h$ , which is determined by the direction of the unit normal vector  $\boldsymbol{\nu}_e$ ,  $e \in \mathcal{E}_h$ . For every polygon  $E$  and edge  $e \in \mathcal{E}_h^E$ , we define a unit normal vector  $\boldsymbol{\nu}_E^e$  that points outside of  $E$ .

We will assume that  $\Omega_h$  is obtained after successive uniform refinements of a given coarse mesh  $\Omega_H$  made of *convex* polygons according to the procedure described in Algorithm 1. Notice that assuming that partitioning a polygonal domain into union of convex subdomains is not restrictive and an algorithm for such decomposition into a small (close to minimum) number of convex polygons is presented in [30].

---

**Algorithm 1** Refinement algorithm, see Figure 1.

---

- 1: **for all** polygons  $E \in \Omega_H$  **do**
- 2:     Introduce the point  $\mathbf{x}_E \in E$  defined as

$$\mathbf{x}_E = \frac{1}{n_E} \sum_{\mathbf{v} \in \mathcal{N}_H^E} \mathbf{x}(\mathbf{v}) ,$$

where  $n_E$  is the number of vertexes  $\mathbf{v}$  of  $E$ , and  $\mathbf{x}(\mathbf{v})$  is the position vector of the vertex  $\mathbf{v}$ .

- 3:     Subdivide  $E$  of  $\Omega_H$  by connecting each midpoint  $\mathbf{v}_m = \mathbf{v}_m(e)$  of each edge  $e \in \mathcal{E}_h^E$  with the point  $\mathbf{x}_E$ , see Figure 1.
  - 4: **end for**
- 

Note that, according to Algorithm 1, the edge midpoints  $\mathbf{v}_m(e)$  and the points  $\mathbf{x}_E$  become additional vertexes in the new mesh  $\Omega_h$ , *i.e.*,

$$\mathcal{N}_h = \mathcal{N}_H \cup \{\mathbf{v}_m(e)\}_{e \in \mathcal{E}_H} \cup \{\mathbf{x}_E\}_{E \in \Omega_H} . \quad (2)$$

The mesh  $\Omega_h$  is also assumed to satisfy the following shape regularity property, which have already been used in [22].

**Assumption 2.1** *There exists an integer number  $N_s$ , independent of  $h$ , such that any polygon  $E \in \Omega_h$  admits a decomposition  $\mathcal{T}_h|_E$  with at most  $N_s$  shape-regular triangles;*

Assumption 2.1 implies the following properties which we use later (cf. [22], for details)

- (M1) The number of vertices and edges of every polygon  $E$  of  $\Omega_h$  is *uniformly* bounded.
- (M2) For every polygon  $E$  and all edges  $e$  of  $E$ , it holds

$$h_E \lesssim h_e \quad h_E^2 \lesssim |E| .$$

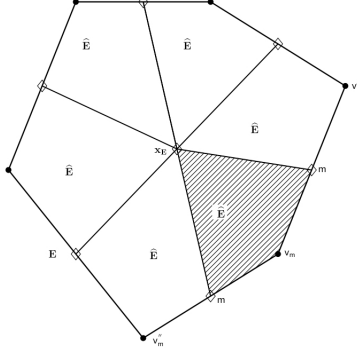


Figure 1: Refinement strategy: coarse element  $E \in \Omega_H$  and sub-elements  $\widehat{E} \in \Omega_h$ . Circles denote the coarse vertexes in  $\mathcal{N}_H$ , while diamonds refer to additional vertexes in  $\mathcal{N}_h$ .

(M3) For every function  $\psi \in H^1(E)$ , the following *trace inequality* holds

$$\|\psi\|_{L^2(e)}^2 \lesssim H_E^{-1} \|\psi\|_{L^2(E)}^2 + H_E |\psi|_{H^1(E)}^2.$$

(M4) For every  $E$  and for every function  $\psi \in H^m(E)$ ,  $m \in \mathbb{N}$ , there exists a polynomial  $\psi_k$  of degree at most  $k$  on  $E$  and such that

$$|\psi - \psi_k|_{H^l(E)} \lesssim H_E^{m-l} |\psi|_{H^m(E)}$$

for all integers  $0 \leq l \leq m \leq k + 1$ .

Note that (M4) follows, for instance, from the Bramble-Hilbert lemma on non star-shaped domains of [34]; a proof related a bit more to the presentation here is also found in [4].

Finally, we assume that the jumps in  $\kappa(x)$  are aligned with the finest grid and we denote by  $\kappa_E$  the coefficient value in the polygon  $E$ .

## 2.2 Mimetic finite difference discretization

To describe the discretization of problem (1), we begin by introducing the discrete approximation space  $V_h$  which is defined as follows. A vector  $v_h \in V_h$  consists of a collection of degrees of freedom  $v_h = \{v_h(\mathbf{v})\}_{\mathbf{v} \in \mathcal{N}_h}$ , where  $v_h(\mathbf{v})$  is a real number associated to the point  $\mathbf{v} \in \mathcal{N}_h$ . To enforce boundary conditions, for all nodes of the mesh which lay on the boundary we set  $v_h(\mathbf{v}) = 0$ , for all  $v_h \in V_h$ , and for all  $\mathbf{v} \in \mathcal{N}_h^\partial$ . Therefore, the dimension of  $V_h$  is equal to the number of internal vertices of the mesh and this space is in fact  $\mathbb{R}^n$ , where  $n$  is the cardinality of  $\mathcal{N}_h^i$ .

We denote by  $a_h(\cdot, \cdot) : V_h \times V_h \rightarrow \mathbb{R}$  the discretization of the bilinear form on the left side of the continuous variational problem (1), defined as follows:

$$a_h(v_h, w_h) = \sum_{E \in \Omega_h} a_h^E(v_h, w_h) \quad \forall v_h, w_h \in V_h,$$

where  $a_h^E(\cdot, \cdot)$  is a symmetric bilinear form on each element  $E$  chosen so that

$$a_h^E(v_h, w_h) \approx \int_E \kappa_E \nabla \tilde{v}_h \cdot \nabla \tilde{w}_h \, d\mathbf{x}.$$

Here,  $\tilde{v}_h$ , and  $\tilde{w}_h$  are functions defined on  $E$  which “extend the data”  $v_h, w_h$  inside the polygon.

To derive a consistent approximation  $a_h^E(\cdot, \cdot)$  we integrate by parts to obtain that

$$\begin{aligned} \int_E \kappa_E \nabla v \cdot \nabla q \, d\mathbf{x} &= -\kappa_E \int_E (\Delta q) v \, d\mathbf{x} + \kappa_E \sum_{e \in \mathcal{E}_h^E} \int_e (\nabla q \cdot \boldsymbol{\nu}_E^e) v \, ds \\ &= \kappa_E \sum_{e \in \mathcal{E}_h^E} \nabla q \cdot \boldsymbol{\nu}_E^e \int_e v \, ds \end{aligned}$$

for all  $v \in H^1(E)$  and for all linear functions  $q$  on  $E$ . Approximating the integral on the right side of the above equation with the trapezoidal rule gives

$$\int_E \kappa_E \nabla v \cdot \nabla q \, d\mathbf{x} \approx \kappa_E \sum_{e \in \mathcal{E}_h^E} (\nabla q \cdot \boldsymbol{\nu}_E^e) h_e \frac{v(\mathbf{v}) + v(\mathbf{v}')}{2},$$

where  $\mathbf{v}$  and  $\mathbf{v}'$  are the two vertexes of  $e \in \mathcal{E}_h^E$ . As shown in [22, 4], the bilinear form  $a_h(\cdot, \cdot)$  can be easily built element by element in a simple algebraic way so that for every piecewise linear vector function  $q$  on  $E$ , and every  $v_h \in V_h$ , we have

$$a_h^E(v_h, q) = \kappa_E \sum_{e \in \mathcal{E}_h^E} (\nabla q \cdot \boldsymbol{\nu}_E^e) h_e \frac{v_h(\mathbf{v}) + v_h(\mathbf{v}')}{2}. \quad (3)$$

Notice that, the meaning of the above is that the discrete bilinear form obeys the standard integration by parts formula when tested with linear functions. With this definition in hand, the mimetic discretization of problem (1) reads: Find  $u_h \in V_h$  such that

$$a_h(u_h, v_h) = (f_h, v_h) \quad \forall v_h \in V_h. \quad (4)$$

The right hand side is defined via its action on  $v_h \in V_h$  as follows

$$(f_h, v_h) = \sum_{E \in \Omega_h} \bar{f}|_E \sum_{\mathbf{v}_i \in \mathcal{N}_h^E} v_h(\mathbf{v}_i) \omega_E^i, \quad (5)$$

where  $\bar{f}|_E$  is the average of  $f$  over  $E$ , and  $\omega_E^i$  are positive weights such that  $\sum_i \omega_E^i = |E|$ . Relation (5) is an approximation to  $\int_\Omega f \tilde{v}_h \, dx$ , which is exact for constant functions  $\tilde{v}_h$ .

Problem (4) can be written as the following linear system of equations

$$A_h u_h = f_h, \quad (6)$$

where  $A_h$  is obviously symmetric. In the next section, we also show it is positive definite as well.

### 2.3 Local bilinear forms

We shall now show that (4) is well posed for a particular choice of mimetic finite difference discretization. Let us recall one way of building the bilinear form  $a_h^E(\cdot, \cdot)$ ; see, e.g., [22, 4]. Let  $E$  be a general polygonal element of  $\Omega_h$ , with  $n_E \geq 3$  vertexes. Then, we need to build a symmetric matrix  $\mathbf{A}_h^E \in \mathbb{R}^{n_E \times n_E}$  which represents the local bilinear form

$$a_h^E(v_h, w_h) = (\mathbf{A}_h^E v_h, w_h) \quad \forall v_h, w_h \in \mathbb{R}^{n_E}.$$

Let  $\mathbf{x} = (x_1, x_2)$  and let  $\rho_1 = 1, \rho_2 = x_1 - x_{1,E}, \rho_3 = x_2 - x_{2,E}$  be a basis for the space of the linear polynomials on  $E$ , with  $\mathbf{x}_E = (x_{1,E}, x_{2,E})$  being the center of mass of  $E$ . Then, we introduce the  $n_E \times 3$  matrix  $\mathbf{N}$  given by

$$\mathbf{N}_{ij} = \rho_j(\mathbf{v}_i) \quad i = 1, \dots, n_E, \quad j = 1, 2, 3,$$

where  $\mathbf{v}_1 = (x_{1,1}, x_{2,1}), \dots, \mathbf{v}_{n_E} = (x_{1,n_E}, x_{2,n_E})$  are the  $n_E$  vertices of the polygon  $E$ , *i.e.*,

$$\mathbf{N} = \begin{pmatrix} 1 & x_{1,1} - x_{1,E} & x_{2,1} - x_{2,E} \\ 1 & x_{1,2} - x_{1,E} & x_{2,2} - x_{2,E} \\ 1 & x_{1,3} - x_{1,E} & x_{2,3} - x_{2,E} \\ \vdots & \vdots & \vdots \\ 1 & x_{1,n_E} - x_{1,E} & x_{2,n_E} - x_{2,E} \end{pmatrix}. \quad (7)$$

Then, it is easy to check that the consistency condition (3) can be expressed as

$$\mathbf{N}^T \mathbf{A}_h^E v_h = \mathbf{R}^T v_h \quad \forall v_h \in \mathbb{R}^{n_E},$$

where the  $n_E \times 3$  matrix  $\mathbf{R}$  with columns  $\mathbf{R}_j, j = 1, 2, 3$ , is the unique matrix that represents the right hand side in (3)

$$\mathbf{R}_j^T v_h = \kappa_E \sum_{\mathbf{e} \in \mathcal{E}_h^E} (\nabla \rho_j \cdot \boldsymbol{\nu}_E^{\mathbf{e}}) \frac{|\mathbf{e}|}{2} (v_h^{\mathbf{v}_1} + v_h^{\mathbf{v}_2}) \quad \forall v_h \in \mathbb{R}^{n_E}.$$

More precisely, for  $i = 1, \dots, n_E$ , let  $\mathbf{e}_i$  be the edge connecting the vertices  $\mathbf{v}_i = (x_{1,i}, x_{2,i})$  and  $\mathbf{v}_{i+1} = (x_{1,i+1}, x_{2,i+1})$  (with the convention that  $\mathbf{v}_{n_E+1} \equiv \mathbf{v}_1$ ), and let  $\boldsymbol{\nu}_E^{\mathbf{e}_i} \in \mathbf{R}^{1 \times 2}$  be the corresponding outward normal vector. Clearly,  $|\mathbf{e}_i| \boldsymbol{\nu}_E^{\mathbf{e}_i} = (x_{2,i+1} - x_{2,i}, x_{1,i} - x_{2,i+1})$ . Therefore, the matrix  $\mathbf{R}$  has the following form

$$\begin{aligned} \mathbf{R} &= \kappa_E \begin{pmatrix} 0 & (|\mathbf{e}_{n_E}| \boldsymbol{\nu}_E^{\mathbf{e}_{n_E}} + |\mathbf{e}_1| \boldsymbol{\nu}_E^{\mathbf{e}_1})/2 \\ 0 & (|\mathbf{e}_1| \boldsymbol{\nu}_E^{\mathbf{e}_1} + |\mathbf{e}_2| \boldsymbol{\nu}_E^{\mathbf{e}_2})/2 \\ 0 & (|\mathbf{e}_2| \boldsymbol{\nu}_E^{\mathbf{e}_2} + |\mathbf{e}_3| \boldsymbol{\nu}_E^{\mathbf{e}_3})/2 \\ \vdots & \vdots \\ 0 & (|\mathbf{e}_{n_E-1}| \boldsymbol{\nu}_E^{\mathbf{e}_{n_E-1}} + |\mathbf{e}_{n_E}| \boldsymbol{\nu}_E^{\mathbf{e}_{n_E}})/2 \end{pmatrix} \\ &= \kappa_E \begin{pmatrix} 0 & (x_{2,2} - x_{2,n_E})/2 & (x_{1,n_E} - x_{1,2})/2 \\ 0 & (x_{2,3} - x_{2,1})/2 & (x_{1,1} - x_{1,3})/2 \\ 0 & (x_{2,4} - x_{2,2})/2 & (x_{1,2} - x_{1,4})/2 \\ \vdots & \vdots & \vdots \\ 0 & (x_{2,1} - x_{2,n_E-1})/2 & (x_{1,n_E-1} - x_{1,1})/2 \end{pmatrix}. \end{aligned}$$

The above construction then provides a matrix representation of the consistency condition

$$\mathbf{A}_h^E \mathbf{N} = \mathbf{R}$$

Moreover, it is easy to check that

$$(\mathbf{R}^T \mathbf{N})_{ij} = (\mathbf{N}^T \mathbf{A}_h^E \mathbf{N})_{ij} = \int_E \kappa_E \nabla \rho_i \cdot \nabla \rho_j \, d\mathbf{x} =: \mathbf{K}_{ij} \quad i, j = 1, 2, 3,$$

with  $\mathbf{K}_{ij}$  clearly equals to  $|E|$  if  $i = j = 2$  or  $i = j = 3$  and zero otherwise, that is,

$$\mathbf{R}^T \mathbf{N} = \kappa_E \begin{pmatrix} 0 & 0 & 0 \\ 0 & |E| & 0 \\ 0 & 0 & |E| \end{pmatrix}.$$

Let  $\mathbf{P} = \mathbf{I} - \mathbf{N}(\mathbf{N}^T \mathbf{N})^{-1} \mathbf{N}^T$  be the orthogonal projection on the  $\text{Range}(\mathbf{N})^\perp$  or, in another words,  $\mathbf{P}$  is the projection on the space orthogonal to the columns of  $\mathbf{N}$ . Then, we set

$$\mathbf{A}_h^E = \frac{1}{|E|} \frac{\mathbf{R} \mathbf{R}^T}{\kappa_E} + s \mathbf{P}, \quad (8)$$

with  $s = \text{trace}(\frac{1}{|E|} \mathbf{R} \mathbf{R}^T) > 0$  is a scaling factor.

We now prove a result which is basic in showing the coercivity, and, thus, solvability of the discrete problem and estimating the condition number of  $\mathbf{A}_h$ .

**Lemma 2.1**  $\mathbf{A}_h^E$  is positive semidefinite. Moreover,  $\mathbf{A}_h^E \mathbf{u} = \mathbf{0}$  if and only if  $\mathbf{u} = (\alpha, \dots, \alpha)^T$  for some  $\alpha \in \mathbb{R}$ .

**Proof** Using that  $\mathbf{P}^2 = \mathbf{P}$  and  $\mathbf{P}^T = \mathbf{P}$ , we have

$$(\mathbf{A}_h^E \mathbf{u}, \mathbf{u}) = \frac{1}{|E| \kappa_E} (\mathbf{R}\mathbf{R}^T \mathbf{u}, \mathbf{u}) + s(\mathbf{P}\mathbf{u}, \mathbf{u}) = \frac{1}{|E| \kappa_E} \|\mathbf{R}^T \mathbf{u}\|^2 + s\|\mathbf{P}\mathbf{u}\|^2, \quad (9)$$

for any  $\mathbf{u} \in \mathbb{R}^3$ . We next show that  $\mathbf{A}_h^E \mathbf{u} = \mathbf{0}$  if and only if  $\mathbf{u} = (\alpha, \dots, \alpha)^T$  for some  $\alpha \in \mathbb{R}$ . One direction of the proof is easy. Indeed, taking  $\mathbf{u} = (\alpha, \dots, \alpha)^T$  for  $\alpha \in \mathbb{R}$ , then

$$\mathbf{u} = \mathbf{N} \begin{pmatrix} \alpha \\ 0 \\ 0 \end{pmatrix},$$

and hence

$$\mathbf{A}_h^E \mathbf{u} = \mathbf{A}_h^E \mathbf{N} \begin{pmatrix} \alpha \\ 0 \\ 0 \end{pmatrix} = \mathbf{R} \begin{pmatrix} \alpha \\ 0 \\ 0 \end{pmatrix} = \mathbf{0}.$$

To prove the other direction, let us assume that  $\mathbf{A}_h^E \mathbf{u} = \mathbf{0}$ . Equation (9) clearly implies that  $\mathbf{R}^T \mathbf{u} = \mathbf{0}$  and  $\mathbf{P}\mathbf{u} = \mathbf{0}$ . From  $\mathbf{P}\mathbf{u} = \mathbf{0}$ , we conclude that  $\mathbf{u} \in \text{Range}(\mathbf{N})$ , and, hence,  $\mathbf{u} = \mathbf{N}\tilde{\mathbf{u}}$  for some  $\tilde{\mathbf{u}} = (\tilde{u}_1, \tilde{u}_2, \tilde{u}_3)^T \in \mathbb{R}^3$ . This yields

$$\mathbf{R}\tilde{\mathbf{u}} = \mathbf{A}_h^E \mathbf{N}\tilde{\mathbf{u}} = \mathbf{A}_h^E \mathbf{u} = \mathbf{0}.$$

We now want to show that  $(\tilde{u}_1, \tilde{u}_2, \tilde{u}_3)^T = (\alpha, 0, 0)^T$  for some  $\alpha \in \mathbb{R}$ . Indeed, the identity  $\mathbf{R}\tilde{\mathbf{u}} = \mathbf{0}$ , shows that  $(\tilde{u}_2, \tilde{u}_3)^T \cdot \boldsymbol{\nu}_E^{\mathbf{e}_i} = 0$  for  $i = 1, \dots, n_E$ . As at least two of the normal vectors  $\{\boldsymbol{\nu}_E^{\mathbf{e}_i}\}_{i=1}^{n_E}$  are linearly independent, this implies that  $\tilde{u}_2 = \tilde{u}_3 = 0$ . Finally, the proof is concluded by setting  $\tilde{u}_1 = \alpha$ ,  $\tilde{u}_2 = \tilde{u}_3 = 0$ , and computing  $\mathbf{N}\tilde{\mathbf{u}}$  which yields  $\mathbf{u} = \mathbf{N}\tilde{\mathbf{u}} = (\alpha, \dots, \alpha)^T$ . To show part one of the thesis, we use that since the kernel of  $\mathbf{A}_h^E$  is made of constant vectors, we have only to show that

$$(\mathbf{A}_h^E \mathbf{u}, \mathbf{u}) > 0,$$

for any non constant vector  $\mathbf{u} = (u_1, u_2, u_3)^T$ . From (9) we clearly have

$$(\mathbf{A}_h^E \mathbf{u}, \mathbf{u}) = \frac{1}{|E| \kappa_E} \|\mathbf{R}^T \mathbf{u}\|^2 + s\|\mathbf{P}\mathbf{u}\|^2 > 0,$$

since  $\|\mathbf{R}^T \mathbf{u}\| \neq \mathbf{0}$  and  $\|\mathbf{P}\mathbf{u}\| \neq \mathbf{0}$  if  $\mathbf{u}$  is a non constant vector.

Setting  $a_{ij}^E = (\mathbf{A}_h^E)_{ij}$ , as a consequence of the second part of Lemma 2.1 we immediately get

$$a_{ii}^E = - \sum_{j:j \neq i} a_{ij}^E.$$

We have then for  $\mathbf{u} \in \mathbb{R}^{n_E}$  and  $\mathbf{v} \in \mathbb{R}^{n_E}$ :

$$\begin{aligned}
\sum_{i,j=1}^{n_E} (-a_{ij}^E)(u_j - u_i)(v_j - v_i) &= \sum_{i,j:i \neq j} (-a_{ij}^E)(u_j - u_i)(v_j - v_i) \\
&= 2 \sum_{i,j:i \neq j} a_{ij}^E u_j v_i - 2 \sum_{i,j:i \neq j} a_{ij}^E u_i v_j \\
&= 2 \sum_{i,j:i \neq j} a_{ij}^E u_j v_i + 2 \sum_{i=1}^{n_E} a_{ii}^E u_i v_i.
\end{aligned}$$

From this identity we get that

$$a_h^E(u_h, v_h) = \frac{1}{2} \sum_{i,j=1}^{n_E} (-a_{ij}^E)(u_{h,i} - u_{h,j})(v_{h,i} - v_{h,j}), \quad (10)$$

where we employ the notation  $u_{h,i} := u_h(\mathbf{v}_i)$ ,  $\mathbf{v}_i \in \mathcal{N}_h^E$ . We note that the sum above is over all  $(i, j)$ ,  $i = 1, \dots, n_E$  and  $j = 1, \dots, n_E$ .

We now introduce (on  $E$ ) a different bilinear form which is spectrally equivalent to  $a_h^E(\cdot, \cdot)$  but the summation is over fewer edges. We will denote this new bilinear form with  $a^E(\cdot, \cdot)$  and define it as

$$a^E(u_h, v_h) = \sum_{E \in \Omega_h} k_E \sum_{e \in \mathcal{E}_h^E} \frac{|E|}{h_e^2} \delta_e(u_h) \delta_e(v_h), \quad (11)$$

where, for every  $e \in \mathcal{E}_h$ , we set  $\delta_e(v_h) = v_h(\mathbf{v}) - v_h(\mathbf{v}')$  being  $\mathbf{v}$  and  $\mathbf{v}'$  the two vertices of the edge  $e$ . Based on (11), we define a global bilinear form on  $V_h$

$$a(u_h, v_h) = \sum_{E \in \Omega_h} a^E(u_h, v_h). \quad (12)$$

We have the following result.

**Lemma 2.2** *The bilinear forms  $a(\cdot, \cdot)$  and  $a_h(\cdot, \cdot)$  are spectrally equivalent with constant depending only on the mesh geometry.*

**Proof** The spectral equivalence is shown first locally on every  $E$ . By Lemma 2.1 we have that  $a_h^E(\cdot, \cdot)$  is symmetric positive semidefinite with one dimensional kernel and therefore,  $a_h(v_h, v_h)$  is a norm on  $\mathbb{R}^{n_E}/\mathbb{R}$ . Same holds for  $a(v_h, v_h)$ , namely, this bilinear form also provides a norm on  $\mathbb{R}^{n_E}/\mathbb{R}$  (as long as the set of edges in  $E$  forms a connected graph). It is easily checked that the entries  $(a_{ij}^E)_{i,j=1}^{n_E}$  and the edge weight in (11) are the same order with respect to  $h_e$  and  $|E|$ . Finally, summing up over all elements  $E$  concludes the proof of the lemma. Clearly, the constants of equivalence depend on the number of edges of the polygons, which is assumed to be bounded by  $N_s$  (see Assumption 2.1).

Lemma 2.2 implies that we can introduce energy norm on  $V_h$  via  $a(\cdot, \cdot)$

$$\|v_h\|_a^2 = \sum_{E \in \Omega_h} k_E |E| \sum_{e \in \mathcal{E}_h^E} \frac{|\delta_e(v_h)|^2}{h_e^2}. \quad (13)$$

We also observe that this energy norm is spectrally equivalent to the energy norm induced by the graph-Laplacian bilinear form  $a_L(\cdot, \cdot)$  (with constants depending on the minimum and maximum values of the coefficient  $k(x)$ ), namely

$$\begin{aligned} a_L(u_h, v_h) &= \sum_{E \in \Omega_h} \sum_{e \in \mathcal{E}_h^E} \delta_e(u_h) \delta_e(v_h), \\ \|v_h\|_{a_L}^2 &= a_L(v_h, v_h) = \sum_{E \in \Omega_h} \sum_{e \in \mathcal{E}_h^E} |\delta_e(v_h)|^2. \end{aligned} \quad (14)$$

As easily seen the graph-Laplacian bilinear form  $a_L(\cdot, \cdot)$  is the same as  $a(\cdot, \cdot)$  when all coefficients  $a_e := k_E |E| / h_e^2$  are set equal to one. To conclude this section, let us mention that in the appendix, Lemma A.1, we prove Poincaré type inequality for the bilinear form in (14), which also gives an estimate on the condition number of  $A_h$ .

**Remark 2.1** *Thanks to the Dirichlet boundary conditions, the quantity  $\|\cdot\|_a$  is a norm on  $V_h$ . For Neumann problem, it this will be only a seminorm. We remark that  $\|\cdot\|_a$  resembles a discrete  $H^1(\Omega)$  norm; indeed, the quantity  $h_h^{-1} \delta_e(v_h)$  represents the tangential component of the gradient on edges and the scalings with respect to  $h_E$  and  $h_e$  give an inner product equivalent to the  $H^1(\Omega)$  on standard conforming finite element spaces.*

In the next section we provide construction of uniform two-level preconditioner for  $a(\cdot, \cdot)$  and prove uniform bound on the condition number of the preconditioned matrix. Thanks to Lemma 2.2 a uniform preconditioner for  $a(\cdot, \cdot)$  will also provide a uniform preconditioner for  $a_h(\cdot, \cdot)$ .

### 3 A Two-Level Preconditioner

In this section we describe a two-level method for preconditioning the linear system of equations (6). In the analysis of the two level preconditioner we denote by  $(\cdot, \cdot)_X$  and  $\|\cdot\|_X$ , respectively the inner product and the norm generated by a symmetric positive definite matrix  $X$ .

The bilinear form  $a(\cdot, \cdot)$  corresponds to the linear system  $Au = f$ , where the operator  $A : V_h \mapsto V_h$  is defined as  $(Au_h, v_h) = a(u_h, v_h)$ . We stress again that in this section we construct preconditioner for  $a(\cdot, \cdot)$ , rather than for  $a_h(\cdot, \cdot)$ , although this is not a restriction, since these two bilinear forms are equivalent (per Lemma 2.2) and a uniform preconditioner for  $a(\cdot, \cdot)$  provides uniform preconditioner for  $a_h(\cdot, \cdot)$  and vice versa.

The bilinear form  $a(\cdot, \cdot)$  can be written in more compact form,

$$a(u_h, v_h) = \sum_{e \in \mathcal{E}_h} a_e \delta_e(u_h) \delta_e(v_h), \quad \text{for all } u_h \in V_h, \quad v_h \in V_h. \quad (15)$$

Here, all coefficients  $a_e$  are positive, as easily seen from the relation defining  $a(\cdot, \cdot)$  in (11) and (12).

Let  $\Omega_H$  be the coarse partition that generated the fine grid through the refinement procedure described in Algorithm 1. Denoting by  $\mathcal{E}_H$  the set of edges of the coarse partition  $\Omega_H$ , and for any  $\mathbf{v}_m = \mathbf{v}_m(e)$ ,  $e \in \mathcal{E}_H$ , let  $\mathbf{v}$  and  $\mathbf{v}'$  be the two endpoints of the edge  $e$ . Let  $V_H \subset V_h$  be the coarse MFD space. Note that  $V_H$  is a subspace of  $V_h$ , and hence we will have to specify the vertex values on the fine partition  $\Omega_h$  of every element of  $V_H$ . This is easy to do by introducing the natural inclusion operator  $I_H^h$ , also known as the prolongation operator, which characterizes the elements from  $V_H$  as elements in  $V_h$ . Its action corresponds to an extension of the coarse grid values to the fine grid vertices by averaging. Denoting by  $\mathcal{N}_H$  the set of all vertices of  $\Omega_H$ , and denoting by  $N_E$  the number of vertices of the element  $E \in \Omega_H$ , for  $I_H^h : V_H \rightarrow V_h$  we have

$$\begin{aligned} (I_H^h v_H)(\mathbf{v}) &= v_H(\mathbf{v}), & \text{for all } \mathbf{v} \in \mathcal{N}_H, \\ (I_H^h v_H)(\mathbf{v}_m(e)) &= \frac{1}{2}(v_H(\mathbf{v}) + v_H(\mathbf{v}')), & \text{for all } \mathbf{v}_m(e), e \in \mathcal{E}_H \\ (I_H^h v_H)(\mathbf{x}_E) &= \frac{1}{N_E} \sum_{\mathbf{v} \in \mathcal{N}_H^E} v_H(\mathbf{v}) & \text{for all } E \in \Omega_H \end{aligned}$$

where the point  $\mathbf{x}_E$  is defined as in Algorithm 1 (see also Figure 2).

We denote by  $\Pi_H : V_h \rightarrow V_H$  the standard interpolation operator, namely, for all  $v_h \in V_h$ , the action  $\Pi_H v_h$  is the element of the coarse space  $V_H$  which has the same value as  $v_h$  at the coarse grid vertices, namely,

$$\Pi_H v_h \in V_H, \quad \text{and} \quad (\Pi_H v_h)(\mathbf{v}) = v_h(\mathbf{v}) \quad \text{for all } \mathbf{v} \in \mathcal{N}_H. \quad (16)$$

There are several different norms on  $V_h$  that we need to use in the analysis. One is the energy norm  $\|\cdot\|_a$  that was already introduced in (13). Further, if  $D$  denotes the diagonal of  $A$ , then we introduce the  $D$ -norm  $\|v\|_D^2 = (Dv_h, v_h)$  for all  $v_h \in V_h$ . This norm is clearly an analogue of a scaled  $L^2$ -norm in finite element analysis. A direct computation shows that

$$(Du_h, v_h) = \sum_{\mathbf{v} \in \mathcal{N}_h} \left( \sum_{e \in \mathcal{E}_h: e \supset \mathbf{v}} a_e \right) u_h(\mathbf{v}) v_h(\mathbf{v}). \quad (17)$$

By Schwarz inequality we easily get the bound

$$\|v_h\|_a \leq c_D \|v_h\|_D \quad \text{for all } v_h \in V_h, \quad (18)$$

and the constant  $c_D$ , by the Gershgorin theorem, can be taken to equal the maximum number of nonzeros per row in  $A$ . On the coarse grid we introduce two types of bilinear forms:

- i)* a restriction of the original form  $a(\cdot, \cdot)$  on  $V_H$ , denoted by  $a_H(\cdot, \cdot) : V_H \times V_H \mapsto \mathbb{R}$ ;
- ii)* a sparser approximation to  $a_H(\cdot, \cdot)$ , which we denote by  $b_H(\cdot, \cdot) : V_H \times V_H \rightarrow \mathbb{R}$ .

The latter bilinear form is build in the same way (11) was built from (10). The formal definitions are as follows:

$$\begin{aligned} (A_H u_H, v_H) &= a(u_H, v_H), \\ (B_H u_H, v_H) &= b_H(u_H, v_H) = \sum_{e \in \mathcal{E}_H} a_{e,H} \delta_e(u_H) \delta_e(v_H). \end{aligned} \quad (19)$$

The main reason to introduce the approximate bilinear form  $b_H(\cdot, \cdot)$  defined in (19) is that this form is much more suitable for computations because the number of nonzeros in the matrix representing  $B_H$  has less nonzeros than in the matrix representing  $A_H$ . To see this, and also to show the spectral equivalence between  $A_H$  and  $B_H$ , we write the restriction of the operator  $A$  on the coarser space in a way that is more suitable for our analysis. First, we split the space of edges  $\mathcal{E}_h$  in subsets of edges on coarse element boundaries and edges interior to the coarse elements,

$$\mathcal{E}_h = \mathcal{E}_m \cup [\cup_{E \in \Omega_H} \mathcal{E}_{0,E}].$$

Here,  $e \in \mathcal{E}_m$  is a subset of  $e_H \in \mathcal{E}_H$ , connecting the mid point of a coarse edge  $e_H$  to the vertices of  $e_H$ . Thus, every  $e_H \in \mathcal{E}_H$  gives two edges in  $\mathcal{E}_m$  or we have

$$\mathcal{E}_m = \cup_{e_H \in \mathcal{E}_H} [e_{H,1} \cup e_{H,2}], \quad \text{where } e_{H,1}, e_{H,2} \in \mathcal{E}_h.$$

Further, for every  $E \in \Omega_H$ ,  $\mathcal{E}_{0,E}$  is the set of edges connecting the mass center of  $E$  with the midpoints of its boundary edges (see Figure 2).

With this notation in hand, we write the restriction of  $A$  on  $V_H$  as follows.

$$\begin{aligned} a_H(u_H, v_H) &= \sum_{e_H \in \mathcal{E}_H} a_{e_H,1} \delta_{e_{H,1}}(u_H) \delta_{e_{H,1}}(v_H) + a_{e_H,2} \delta_{e_{H,2}}(u_H) \delta_{e_{H,2}}(v_H) \\ &\quad + \sum_{E \in \Omega_H} \sum_{e \in \mathcal{E}_{0,E}} a_e \delta_e(u_H) \delta_e(v_H) \\ &= \frac{1}{2} \sum_{e \in \mathcal{E}_H} \tilde{a}_e \delta_e(u_H) \delta_e(v_H) + \sum_{E \in \Omega_H} \sum_{e \in \mathcal{E}_{0,E}} a_e \delta_e(u_H) \delta_e(v_H), \end{aligned} \quad (20)$$

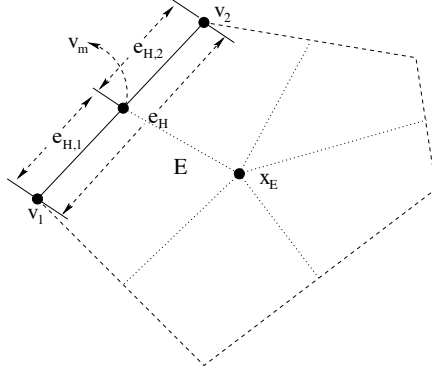


Figure 2: A coarse element; boundary and internal edges.

where  $\tilde{a}_e = (a_{e_{H,1}} + a_{e_{H,2}})$ . In addition, for any fixed element  $E \in \Omega_H$ , we obtain

$$\begin{aligned} \sum_{e \in \mathcal{E}_{0,E}} a_e \delta_e(u_H) \delta_e(v_H) &= \\ &= \sum_{e \in \mathcal{E}_{0,E}} \frac{1}{n_E} \sum_{e' \in \mathcal{E}_{0,E}} a_e (u_H(\mathbf{v}_m) - u_H(\mathbf{v}'_m)) (v_H(\mathbf{v}_m) - v_H(\mathbf{v}'_m)) \end{aligned} \quad (21)$$

where we denote by  $\mathbf{v}'_m$  the midpoint of  $e'$ . This identity follows from the fact that each of  $u_H(\mathbf{x}_E)$  is an average of vertex values which is actually equal to the average of midpoint values for  $u_H \in V_H$  and  $v_H \in V_H$ .

Finally, in the definition of the two-level preconditioner we need the  $\ell^2$  orthogonal projection  $Q_H$  onto the space  $V_H$ , *i.e.*,

$$(Q_H v_h, v_H) = (v_h, v_H) \quad \forall v_H \in V_H.$$

The (symmetrized) two-grid iteration method computes for any given initial iterate  $u^0$  a two-grid iterate  $u^{TG}$  as described in Algorithm 2 where  $R$  denotes a suitable smoothing operator.

---

**Algorithm 2** Two-level algorithm:  $u^{TG} \leftarrow u^0$

---

- 1: *Pre-smoothing*:  $v = u^0 + R^T(f - Au^0)$ ;
  - 2: *Coarse-grid correction*:  $e_H = B_H^{-1} Q_H(f - Av)$ ,  $w = v + e_H$ ;
  - 3: *Post-smoothing*:  $u^{TG} = w + R(f - Aw)$ .
- 

The error propagation operator  $E$  associated with this algorithm satisfies the relation

$$E = (I - RA)(I - B_H^{-1} Q_H A)(I - R^T A).$$

A usual situation is when  $E$  is a uniform contraction in  $\|\cdot\|_a$ -norm. This is definitely the case when  $B_H = A_H$ . A proof of this fact follows the same

lines as the proof for the case  $B_H \neq A_H$  which we present below. In the case  $B_H = A_H$  the operator  $E$  is a contraction because  $(I - A_H^{-1}Q_H A)$  is an  $A$ -orthogonal projection and therefore non-expansive in  $\|\cdot\|_A$ -norm and, in addition,  $(I - RA)$  is a contraction in  $\|\cdot\|_A$  norm.

However, when the coarse grid matrix is approximated, *i.e.* we have  $B_H \neq A_H$ , then the error propagation operator does not have to be a contraction and we aim to bound the condition number of the preconditioned system. In order to show uniform bounds on the condition number of the system preconditioned by the two level MFD preconditioner it is useful to consider its explicit form given by  $B^{-1} = (I - E)A^{-1}$ , or,

$$B^{-1} = \tilde{R} + (I - AR^T)B_H^{-1}Q_H(I - RA). \quad (22)$$

As is well known (see [47, pp.67-68] and [37]), if  $\|I - RA\|_A < 1$  then the preconditioner  $B$  is symmetric and positive definite. Such statement follows from the canonical form of the multiplicative preconditioner as given in [47, Theorem 3.15, pp. 68-69] and [32].

**Theorem 3.1 (Theorem 3.15 in [47])** *The following identity holds for the two level preconditioner  $B$ , given by (22)*

$$(Bv, v) = \min_{v_H \in V_H} \left( \|v_H\|_{B_H}^2 + \|v - (I - R^T A)v_H\|_{\tilde{R}^{-1}}^2 \right). \quad (23)$$

What we will do next is to use this theorem and derive spectral equivalence results for  $B$  and  $A$ .

### 3.1 Smoother: assumptions and properties

For the smoother  $R$  we assume that it is nonsingular operator and convergent in  $\|\cdot\|_a$ -norm, that is,

$$\|I - RA\|_a^2 \leq 1 - \delta_R < 1.$$

This implies that the operator  $D_R = (R^{-1} + R^{-T} - A)$  is symmetric and positive definite and also the so called symmetrizations of  $R$ , namely  $\tilde{R} = R^T D_R R$  and  $\tilde{R} = R D_R R^T$  are also symmetric and positive definite. Denoting with  $D$  the diagonal of  $A$ , we make the following assumptions:

**Assumption 3.1** *We assume that in the case of nonsymmetric smoother,  $R \neq R^T$ , the following inequality holds with  $D_R = (R^{-1} + R^{-T} - A)$  and  $D$ , the diagonal of  $A$ :*

$$(D_R v, v) \lesssim (Dv, v).$$

We note that we made this assumption only for a nonsymmetric smoother  $R \neq R^T$ . This assumption is easily verified for Gauss-Seidel or SOR smoother. For example, in the case of Gauss-Seidel smoother we have  $D_R = D$  and for SOR method with relaxation parameter  $\omega \in (0, 2)$  we have  $D_R = \frac{2-\omega}{\omega} D$ .

The next assumption is a typical assumption in the multigrid methods (see [35], [19]) and is as follows.

**Assumption 3.2** Let  $\tilde{R}$  be the symmetrization of  $R$  and  $D$  let be the diagonal of  $A$ . We assume that

$$(Dv, v) \lesssim (\tilde{R}v, v)$$

Such assumption is easily verified for Gauss-Seidel method, SOR or Schwarz smoothers (see [49, 47]), and also for polynomial smoothers as well (see [40]).

### 3.2 Coarse grid approximation properties

To study the spectral equivalence between the preconditioner defined by the two level method and  $A$  we need several auxiliary results which are the subject of the next two Lemmas. The first result is an approximation property and is instrumental in the analysis.

**Lemma 3.1** For every  $v_h \in V_h$  we have

$$\|v_h - \Pi_H v_h\|_D^2 \leq c_I \|v_h\|_a^2 \quad (24)$$

for a positive constant  $c_I$  independent of  $v_h$ .

**Proof** For  $v_h \in V_h$  we have that

$$\begin{aligned} (v_h - \Pi_H v_h)(\mathbf{v}_m) &= v_h(\mathbf{v}_m) - \frac{1}{2}(v_h(\mathbf{v}) + v_h(\mathbf{v}')) \\ &= \frac{1}{2}(v_h(\mathbf{v}_m) - v_h(\mathbf{v})) + \frac{1}{2}(v_h(\mathbf{v}_m(e)) - v_h(\mathbf{v}')). \end{aligned} \quad (25)$$

Analogously, we obtain

$$\begin{aligned} (v_h - \Pi_H v_h)(\mathbf{x}_E) &= v_h(\mathbf{x}_E) - \frac{1}{n_E} \sum_{\mathbf{v} \in \mathcal{N}_h^E} \Pi_H v_h(\mathbf{v}) \\ &= \sum_{\mathbf{v} \in \mathcal{N}_h^E} \frac{1}{n_E} (v_h(\mathbf{x}_E) - v_h(\mathbf{v})). \end{aligned} \quad (26)$$

Next, we use (25)-(26) and the definition of  $\|\cdot\|_D$  given in (17). Splitting the sum over  $\mathbf{v} \in \mathcal{N}_h$  in accordance with (2) into: (1) a sum over the midpoints of coarse edges; and (2) sum over mass centers of coarse elements; and recalling that  $(v_h - \Pi_H v_h)(\mathbf{v}) = 0$  for  $\mathbf{v} \in \mathcal{N}_H$  then gives

$$\begin{aligned} \|v_h - \Pi_H v_h\|_D^2 &= \sum_{\mathbf{v} \in \mathcal{N}_h} \left( \sum_{e \in \mathcal{E}_h; \mathbf{v} \in e} a_e \right) [(v_h - \Pi_H v_h)(\mathbf{v})]^2 \\ &= \frac{1}{2} \sum_{e_H \in \mathcal{E}_H} (a_{e_{H,1}} + a_{e_{H,2}}) (\delta_{e_{H,1}}(v_h) + \delta_{e_{H,2}}(v_h))^2 \\ &\quad + \sum_{E \in \Omega_H} \frac{1}{n_E} \left( \sum_{e' \in \mathcal{E}_{0,E}} a_{e'} \right) \sum_{e \in \mathcal{E}_{0,E}} [\delta_e(v_h)]^2 \\ &\leq c_I \|v_h\|_a^2. \end{aligned} \quad (27)$$

The proof is complete.

### 3.3 Spectral equivalence result

In this section we prove that the preconditioner given by the multiplicative two level MFD algorithm is spectrally equivalent to the operator  $A$ .

**Lemma 3.2** *For every  $v_h \in V_h$  the following inequalities hold with positive constants  $c_I, c_s, c_1$ , and  $c_2$  independent of  $v_h \in V_h$  and  $v_H \in V_H$*

- (i)  $\|\Pi_H v_h\|_a \leq c_s \|v_h\|_a$ ;
- (ii)  $(Av_h, v_h) \leq (\tilde{R}^{-1}v_h, v_h)$ ;
- (iii)  $(R\tilde{R}^{-1}R^T Av_h, Av_h) \leq C_R \|v_h\|_a$ ;
- (iv)  $c_1^{-1}(B_H v_H, v_H) \leq (A_H v_H, v_H) \leq c_2(B_H v_H, v_H)$ .

**Proof** We prove (i) by using the inequality (18) and the approximation property proved in Lemma 3.1

$$\begin{aligned} \|\Pi_H v_h\|_a &\leq \|v_h - \Pi_H v_h\|_a + \|v_h\|_a \\ &\leq c_D \|v_h - \Pi_H v_h\|_D + \|v_h\|_a \leq (1 + c_I c_D) \|v_h\|_a. \end{aligned}$$

The proof of (ii) follows from the following implications

$$\begin{aligned} 0 \leq \|(I - RA)v_h\|_A^2 &\implies 0 \leq ((I - \tilde{R}A)v_h, v_h)_A \implies \\ (\tilde{R}Av_h, Av_h) \leq (Av_h, v_h) &\implies (A^{1/2}\tilde{R}A^{1/2}v_h, v_h) \leq (v_h, v_h) \implies \\ (v_h, v_h) \leq (A^{-1/2}\tilde{R}^{-1}A^{-1/2}v_h, v_h) &\implies (Av_h, v_h) \leq (\tilde{R}^{-1}v_h, v_h). \end{aligned}$$

The proof of (iii) is as follows. If the smoother is symmetric, that is,  $R = R^T$  we have with  $X = A^{1/2}RA^{1/2}$  and  $w_h = A^{1/2}v_h$ :

$$(R\tilde{R}^{-1}R^T Av_h, v_h)_A = ((2I - X)^{-1}Xw_h, w_h) \leq (w_h, w_h) = \|v_h\|_A^2.$$

We used above that  $\|X\| < 1$  and that  $\frac{t}{2-t} \in [0, 1]$  for  $t \in [0, 1]$ . For the nonsymmetric smoothers, the estimate follows from Assumption 3.1

$$\begin{aligned} (R\tilde{R}^{-1}R^T Av_h, v_h)_A &= (D_R^{-1}Av_h, Av_h) \leq (A^{1/2}D^{-1}A^{1/2}w_h, w_h) \\ &\leq \rho(A^{1/2}D^{-1}A^{1/2})(w_h, w_h) \\ &= \rho(D^{-1/2}AD^{-1/2})\|v_h\|_A^2 = c_R \|v_h\|_A^2. \end{aligned}$$

Finally, (iv) follows by using the formulae given in (21) and (20) and proceeding as in the proof of Lemma 2.2. Note that to prove the spectral equivalence we need to only estimate the second term on the right side of (20) (or equivalently the term on the right side of (21)). This is straightforward using the fact that all norms in a finite dimensional space are equivalent.

In the proof we used (21) and (20) to show that  $a_H(\cdot, \cdot)$  and  $b_H(\cdot, \cdot)$  are equivalent. We remark that to achieve that, the coefficients  $a_{e,H}$  of the coarse grid bilinear form  $b_H(\cdot, \cdot)$  in (19) can be all set to one. Then the equivalence constants in Lemma 3.2 will depend on the variations in the coefficient  $k(x)$ . However, other choices are also possible. One such choice is minimizing the Frobenius norm of the difference of the local matrices for  $b_H(\cdot, \cdot)$  and  $a_H(\cdot, \cdot)$ . For more details on such approximations that use the so called edge matrices we refer to [39].

Using the canonical representation for  $B$  given in (23) we prove the following uniform preconditioning result.

**Theorem 3.2** *The condition number of  $BA$  satisfies*

$$\kappa(BA) \leq 2 \max\{1, c_2\}(c_1 c_s + 2c_I + 2c_s).$$

**Proof** In this proof, we use the Assumptions 3.1-3.2 and Lemma 3.1 and Lemma 3.2. We first show the lower bound. For any  $v_h \in V_h$  and  $v_H \in V_H$  we have

$$\begin{aligned} \|v_h\|_A^2 &\leq 2\|v_h - (I - R^T A)v_H\|_A^2 + 2\|(I - R^T A)v_H\|_A^2 \\ &\leq 2\|v_h - (I - R^T A)v_H\|_{\tilde{R}^{-1}}^2 + 2\|v_H\|_{A_H}^2 \\ &\leq 2 \max\{1, c_2\}[\|v_h - (I - R^T A)v_H\|_{\tilde{R}^{-1}}^2 + \|v_H\|_{B_H^{-1}}^2]. \end{aligned}$$

Taking the minimum over all  $v_h \in V_h$  then shows that

$$(Av_h, v_h) \leq 2 \max\{1, c_2\}(B^{-1}v_h, v_h).$$

For the upper bound, we choose  $v_H = I_H^h v_h$  and we have

$$\begin{aligned} (B^{-1}v_h, v_h) &\leq c_1 \|I_H^h v_h\|_A^2 + 2\|v_h - I_H^h v_h\|_{\tilde{R}^{-1}}^2 + 2\|R^T A I_H^h v_h\|_{\tilde{R}^{-1}}^2 \\ &\leq c_1 c_s \|v_h\|_A^2 + 2c_I \|v_h\|_A^2 + 2\|I_H^h v_h\|_A^2 \\ &\leq (c_1 c_s + 2c_I + 2c_s)(Av_h, v_h). \end{aligned}$$

The proof is complete.

**Remark 3.1** *We remark, that a multilevel extension of the results presented here is possible via the auxiliary (fictitious) space framework (since the bilinear forms are modified). We refer to [48] [45] and [36, Section 2]) for the relevant techniques that allow the extension of the results presented here to the multilevel case.*

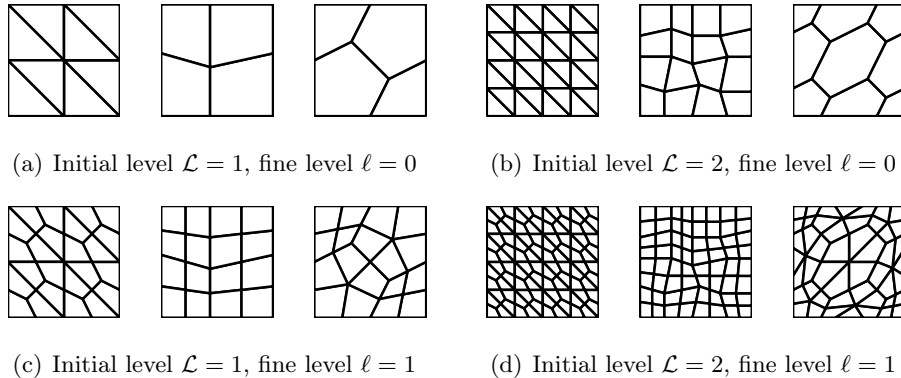


Figure 3: Top: *Tria*, *Quad* and *Hex* meshes with initial levels  $\mathcal{L} = 1$  (left) and  $\mathcal{L} = 2$  (right) and fine level  $\ell = 0$ . Bottom: corresponding grids obtained after a uniform refinement ( $\ell = 1$ ) employing the refinement strategy of Section 3.

## 4 Numerical Results

We are interested in approximating the solution of the elliptic problem (1) on the unit square, where the right hand side is chosen so that the analytical solution is given by

$$u(x_1, x_2) = x_1(x_2 - x_2^2) \exp(x_2) \cos\left(\frac{\pi x_1}{2}\right).$$

We start from the initial grids of levels  $\mathcal{L} = 1, 2$  shown in Figure 3 (top), that we denote by *Tria*, *Quad* and *Hex* meshes, respectively. Starting from these initial grids, we test our two-level solver on a sequence of finer grids constructed by employing the refinement strategy described in Section 3. More precisely, at each further step of refinement  $\ell = 1, 2, \dots$  we consider a uniform refinement of the grid at the previous level obtained employing the refinement strategy described in Section 3, cf. Figure 3 (bottom) for  $\ell = 1$ , *i.e.*, the meshes obtained after one level of refinement. As pre-smoother we employ  $\nu$  steps of the Gauss-Seidel iterative algorithm, while a direct solver is employed to solve the coarse problem. All simulations are performed by using the null vector as initial guess, and we use as stopping criterium  $\|\mathbf{r}^{(k)}\| \leq 10^{-9} \|\mathbf{b}\|$ , being  $\mathbf{r}^{(k)}$  the residual at the  $k$ -th iteration,  $\mathbf{b}$  the right-hand side of the linear system, and  $\|\cdot\|$  the Euclidean norm.

In Table 1 we report, starting from the initial grids shown in Figure 3 with  $\ell = 0$ , and  $\mathcal{L} = 1$ , the iteration counts of our two-level algorithm when varying the fine refinement level  $\ell$ . This set of experiments has been obtained with  $\nu = 2$  pre-smoothing steps. We clearly observe that our solver seems to be robust as the mesh size goes to zero: indeed the iteration counts are

	it.	$\rho$	$\mathcal{K}(\mathbf{A})$	rate	it.	$\rho$	$\mathcal{K}(\mathbf{A})$	rate	it.	$\rho$	$\mathcal{K}(\mathbf{A})$	rate
$\ell = 1$	18	0.3	1.1e+1	-	9	0.1	5.9e+0	-	7	0.1	6.9e+0	-
$\ell = 2$	13	0.2	4.9e+1	2.2	8	0.1	2.6e+1	2.1	8	0.1	3.2e+1	2.2
$\ell = 3$	18	0.1	2.2e+2	2.1	8	0.1	1.1e+2	2.0	10	0.1	1.4e+2	2.1
$\ell = 4$	22	0.4	9.2e+2	2.1	9	0.1	4.2e+2	2.0	11	0.1	6.2e+2	2.1
$\ell = 5$	23	0.4	3.9e+3	2.0	9	0.1	1.7e+3	2.0	12	0.2	1.1e+4	2.1
	<i>Tria</i> grids				<i>Quad</i> grids				<i>Hex</i> grids			

Table 1: Iteration counts of the two-level algorithm and computed convergence factor  $\rho$  for different fine refinement level  $\ell$  starting from the initial grids of in Figure 3 with  $\mathcal{L} = 1$ . For completeness, the condition number of the stiffness matrix  $\mathcal{K}(\mathbf{A})$  and its growth rate are also reported. Number of pre-smoothing steps  $\nu = 2$ .

almost independent of the size of the problem. In Table 1 we also show the computed convergence factor

$$\rho = \exp\left(\frac{1}{n} \log \frac{\|\mathbf{r}^{(n)}\|}{\|\mathbf{r}^{(0)}\|}\right), \quad (28)$$

where  $n$  is the number of iterations needed to achieve convergence. Finally, for completeness, we have also computed the condition number of the stiffness matrix  $\kappa(\mathbf{A})$  as well as its growth rate (cf. Table 1). As expected, we can clearly observe that the condition number increases quadratically as the mesh is refined.

We have repeated the same set of experiments starting from the initial grids depicted in Figure 3 with  $\mathcal{L} = 2$  and  $\ell = 0$ . The computed results are reported in Table 2. Notice that, in this case, on *Hex*-type grids the condition number seems to grows slightly faster than expected. Next, we address the influence of the number of smoothing steps of the performance of our two-level solver. In Table 3 we report the iteration counts when increasing the number of pre-smoothing steps  $\nu = 3, 4, 5$ . The results shown in Table 3 have been obtained starting from the initial grids of Figure 3 with  $\mathcal{L} = 1$  and  $\ell = 0$ ; the corresponding ones obtained with the initial grids of Figure 3,  $\mathcal{L} = 2$  and  $\ell = 0$  are completely analogous and are not reported here, for the sake of brevity. From the iteration counts reported in Table 3 we can conclude that (i) in all the cases considered, our two-level method is robust as the mesh size is refined; (ii) as expected, the performance of the algorithm improves as the number of smoothing steps increases.

	it.	$\rho$	$\mathcal{K}(\mathbf{A})$	rate	it.	$\rho$	$\mathcal{K}(\mathbf{A})$	rate	it.	$\rho$	$\mathcal{K}(\mathbf{A})$	rate
$\ell = 1$	16	0.3	4.3e+1	-	8	0.1	2.7e+1	-	7	0.1	1.3e+1	-
$\ell = 2$	14	0.2	2.0e+1	2.2	9	0.1	1.1e+2	2.1	14	0.2	6.5e+1	2.4
$\ell = 3$	17	0.2	8.6e+2	2.1	10	0.1	4.6e+2	2.0	18	0.3	3.3e+2	2.4
$\ell = 4$	21	0.4	3.7e+3	2.1	10	0.1	1.9e+3	2.0	22	0.4	2.1e+3	2.6
	<i>Tria</i> grids				<i>Quad</i> grids				<i>Hex</i> grids			

Table 2: Iteration counts of the two-level algorithm and computed convergence factor  $\rho$  for different fine refinement levels  $\ell$  starting from the coarse grids of in Figure 3 with  $\mathcal{L} = 2$ . For completeness, the condition number of the stiffness matrix  $\mathcal{K}(\mathbf{A})$  and its growth rate are also reported. Number of pre-smoothing steps  $\nu = 2$ .

	$\nu = 3$	$\nu = 4$	$\nu = 5$	$\nu = 3$	$\nu = 4$	$\nu = 5$	$\nu = 3$	$\nu = 4$	$\nu = 5$
$\ell = 1$	11	9	8	7	6	5	6	6	5
$\ell = 2$	10	9	8	7	6	6	7	6	6
$\ell = 3$	11	11	9	7	6	6	8	7	7
$\ell = 4$	15	12	10	7	6	6	8	8	7
$\ell = 5$	16	13	11	7	6	6	9	8	7
	<i>Tria</i> grids			<i>Quad</i> grids			<i>Hex</i> grids		

Table 3: Iteration counts as a function of the number of pre-smoothing steps  $\nu = 3, 4, 5$  and for different fine refinement levels  $\ell$  starting from the initial grids of Figure 3,  $\mathcal{L} = 1$ .

Finally, we demonstrate numerically that our scheme also provides a uniform preconditioner, that is the number of PCG iterations needed to achieve convergence up to a (user-defined) tolerance is uniformly bounded independently of the number of degrees of freedom whenever CG is accelerated by the preconditioner described in Section 3. In Table 4 we report the PCG iteration counts as a function of the number of the fine level  $\ell = 1, 2, 3, 4, 5$  starting from the initial grids shown in Figure 3 ( $\mathcal{L} = 1, 2$ ,  $\ell = 0$ ) for *Hex*-type grids. For completeness, we also report the computed convergence factor  $\rho$  (second and fifth columns) and the corresponding CG iteration counts needed to solve the unpreconditioned system (third and sixth columns). It is clear that

employing our preconditioner leads to a uniformly bounded number of iterations (independent of the characteristic size of the underlying partition). On the other hand, the iteration counts needed to solve the unpreconditioned systems grows linearly as the mesh size goes to zero.

	PCG it.	$\rho$	CG it.	PCG it.	$\rho$	CG it.
$\ell = 1$	10	0.25	19	11	0.27	30
$\ell = 2$	12	0.29	42	10	0.25	66
$\ell = 3$	10	0.23	92	10	0.23	133
$\ell = 4$	10	0.23	210	10	0.24	324
$\ell = 5$	10	0.25	533	-	-	-
	$\mathcal{L} = 1$			$\mathcal{L} = 2$		

Table 4: PCG iteration counts and computed convergence factor  $\rho$  as a function of the number of level  $\ell$  starting from the initial grids of Figure 3,  $\mathcal{L} = 1, 2$ , *Hex* grids. For comparison, the CG iteration counts needed to solve the unpreconditioned systems are also reported.

## 5 Conclusions

We have proposed and analyzed a two level preconditioner for the mimetic finite difference discretization of elliptic equation. Our preconditioner uses inexact coarse grid solver (non-inherited coarse grid bilinear form) and results in optimal method with sparser coarse grid operators. We proved that the condition number of the preconditioned system is uniformly bounded. We also implemented the preconditioner and verified numerically the theoretical results.

## 6 Acknowledgements

Part of this work was completed while the third author was visiting MOX at Politecnico di Milano in 2013. Thanks go to the MOX for the hospitality and support. The work of the first and second author has been partially founded by the 2013 GNCS project “*Aspetti emergenti nello studio di strategie adattative per problemi differenziali*”. The research of the third author was supported in part by NSF grant DMS-1217142, and Lawrence Livermore National Laboratory through subcontract B603526.

## A Poincaré-type inequality

We now give a lower bound of the Poincaré constant and the condition number of the MFD matrix. We estimate the Cheeger's constant (see [31]) for the graph corresponding to the MFD and our considerations closely follow [38, 33]. Below we do not consider any boundary conditions on our vectors from  $V_h$  and remark that the case when we have boundary conditions is included in the proof (for details see [31]). In the following, for the ease of presentation, we omit the subscript  $h$  on the vectors/functions, namely, we shall use  $u, v$  and  $w$  instead of  $u_h, v_h$  and  $w_h$ .

The graph Laplacian is defined in (14) and we recall the definition here,

$$(\mathcal{L}u, v) = a_L(u, v) = \sum_{e \in \mathcal{E}_h} \delta_e(u) \delta_e(v) \quad \text{for all } u \in V_h, \quad v \in V_h.$$

The smallest eigenvalue of  $\mathcal{L}$  is  $\lambda_1 = 0$  with eigenvector  $w_1 = \mathbf{1} = (1, \dots, 1)^T$ . We denote by  $\lambda_2$  the minimum, nonzero eigenvalue of  $\mathcal{L}$ , that is

$$\lambda_2 = \inf_{z \in V_h, (z, \mathbf{1})=0} \frac{\langle \mathcal{L}z, z \rangle}{(z, z)}. \quad (29)$$

Let  $w \in V_h$  be one of the eigenvectors corresponding to  $\lambda_2$ , that is,  $w$  satisfies

$$\langle \mathcal{L}w, v \rangle = \lambda_2(w, v) \quad \text{for all } v_h \in V_h. \quad (30)$$

For every  $v \in V_h$  we define  $v^+$  as

$$v^+(\mathbf{v}) = \begin{cases} v(\mathbf{v}) & \text{if } v(\mathbf{v}) \geq 0 \\ 0 & \text{otherwise.} \end{cases} \quad (31)$$

Accordingly, we define  $v^-$  such that  $v^- = v^+ - v$ . The following result provides a lower bound for the minimum eigenvalue  $\lambda_2$ .

**Lemma A.1** *Let  $w \in V_h$  be an eigenvector of  $\mathcal{L}$  corresponding to  $\lambda_2$ . Then*

$$\lambda_2 \geq \frac{(\mathcal{L}w^+, w^+)}{(w^+, w^+)}. \quad (32)$$

**Proof** From (30) we have

$$\langle \mathcal{L}w, w^+ \rangle = \lambda_2(w, w^+).$$

We note that

$$(w, w^+) = (w^+, w^+) \quad \text{and} \quad (\mathcal{L}w, w^+) = (\mathcal{L}w^+, w^+) - (\mathcal{L}w^-, w^+).$$

A simple calculation shows that

$$(\mathcal{L}w^-, w^+) = - \sum_{\{\mathbf{v}_1, \mathbf{v}_2\} \in \mathcal{E}_h^\pm} |w(\mathbf{v}_1)w(\mathbf{v}_2)|$$

where  $\mathcal{E}_h^\pm = \{\{\mathbf{v}_1, \mathbf{v}_2\} \in \mathcal{E}_h : w(\mathbf{v}_1)w(\mathbf{v}_2) \leq 0\} \subseteq \mathcal{E}_h$ . Hence, we have

$$\lambda_2 = \frac{(\mathcal{L}w, w^+)}{(w, w^+)} = \frac{(\mathcal{L}w^+, w^+) + |(\mathcal{L}w^-, w^+)|}{(w^+, w^+)} \geq \frac{(\mathcal{L}w^+, w^+)}{(w^+, w^+)},$$

which completes the proof.

Let  $\mathcal{S}$  be a subset of  $\mathcal{N}_h$  and  $\bar{\mathcal{S}} = \mathcal{N}_h \setminus \mathcal{S}$ . We denote by  $\mathcal{E}(\mathcal{S}, \bar{\mathcal{S}})$  the set of edges with one endpoint in  $\mathcal{S}$  and the other in  $\bar{\mathcal{S}}$ . We define the Cheeger constant  $C_c$  for  $\Omega_h$  as follows

$$C_c = \min_{\mathcal{S} \subset \mathcal{N}_h} \frac{|\mathcal{E}(\mathcal{S}, \bar{\mathcal{S}})|}{\min(|\mathcal{S}|, |\bar{\mathcal{S}}|)}, \quad (33)$$

where  $|\mathcal{S}|$  and  $|\mathcal{E}(\mathcal{S}, \bar{\mathcal{S}})|$  denote the cardinality of  $\mathcal{S}$  and  $\mathcal{E}(\mathcal{S}, \bar{\mathcal{S}})$ , respectively.

The Cheeger's constant provide We are ready to prove the following Poincaré-type inequality.

**Proposition A.1** *Let  $C_c$  be the Cheeger constant associated to the partition  $\Omega_h$ . Then there holds*

$$C_c^2(v, v) \leq (\mathcal{L}v, v) \quad (34)$$

for every  $v \in V_h$ .

**Proof** From Lemma A.1 we have for all  $v \in V_h$ ,

$$\frac{(\mathcal{L}v, v)}{(v, v)} \geq \lambda_2 \geq \frac{(\mathcal{L}w^+, w^+)}{(w^+, w^+)}. \quad (35)$$

We relabel the vertices of  $\Omega_h$  according to the eigenvector  $w$  so that  $w(\mathbf{v}_i) \leq w(\mathbf{v}_{i+1})$  for  $i = 1, \dots, (N_h - 1)$ , where  $N_h = |\mathcal{N}_h|$  is the cardinality of  $\mathcal{N}_h$ . Then, for every  $1 \leq i \leq N_h$  we consider the set

$$C_i = \{(\mathbf{v}_j, \mathbf{v}_k) \in \mathcal{E}_h : 1 \leq j \leq i < k \leq N_h \}$$

and we define

$$\alpha = \min_{1 \leq i \leq N_h} \frac{|C_i|}{\min(1, N_h \setminus \{i\})}.$$

It is clear that  $\alpha \geq C_c$ . Setting  $\mathcal{N}_h^+ = \{\mathbf{v} \in \mathcal{N}_h : w(\mathbf{v}) \geq 0\}$  and denoting by  $\mathcal{E}^+ \subseteq \mathcal{E}$  the set of edges  $e = \{\mathbf{v}_1, \mathbf{v}_2\}$  with  $\mathbf{v}_1, \mathbf{v}_2 \in \mathcal{N}_h^+$  and by  $\sigma_e(v) = (v(\mathbf{v}_1) + v(\mathbf{v}_2))$  yield

$$\begin{aligned} \frac{(\mathcal{L}w^+, w^+)}{(w^+, w^+)} &= \frac{\sum_{e \in \mathcal{E}^+} [\delta_e(w^+)]^2}{\sum_{\mathbf{v} \in \mathcal{N}_h} [w^+(\mathbf{v})]^2} = \frac{\sum_{e \in \mathcal{E}^+} [\delta_e(w^+)]^2 \sum_{e \in \mathcal{E}^+} [\sigma_e(w^+)]^2}{\sum_{\mathbf{v} \in \mathcal{N}_h} w_h^+(\mathbf{v})^2 \sum_{e \in \mathcal{E}^+} [\sigma_e(w^+)]^2} \\ &\geq \frac{\left(\sum_{e \in \mathcal{E}_h} \delta_e([w^+]^2)\right)^2}{4 \sum_{\mathbf{v} \in \mathcal{N}_h} w^+(\mathbf{v})^2} \geq \frac{\left(\sum_{i=1}^{N_h-1} (w_h^2(\mathbf{v}_{i+1}) - w_h^2(\mathbf{v}_i)) |C_i|\right)^2}{4 \sum_{\mathbf{v} \in \mathcal{N}_h} w_h^+(\mathbf{v})^2} \\ &\geq \frac{\left(\sum_{i=1}^{N_h-1} (w_h^2(\mathbf{v}_{i+1}) - w_h^2(\mathbf{v}_i)) i \alpha\right)^2}{4 \sum_{\mathbf{v} \in \mathcal{N}_h} w_h^+(\mathbf{v})^2} \geq \alpha^2 \geq C_c^2. \end{aligned}$$

Combining the above result with (35) yields the result.

It is straightforward to prove the following estimate. We then have the following corollary.

**Corollary A.1** *We have the following estimate on the condition number of  $\mathcal{L}$ :*

$$C_c^2 \leq \frac{(\mathcal{L}v, v)}{(v, v)} \leq C_z \quad (36)$$

for every  $v \in V_h$ , where  $C_z = \max_{\mathbf{v}} |\{e \in \mathcal{E}_h \mid e \supset \mathbf{v}\}|$

To conclude, let us mention that for finite difference or finite element meshes one can obtain a quantitative estimate on  $C_c$ . In  $d$ -spatial dimensions we have

$$\min_{\mathcal{S}, \bar{\mathcal{S}}} |\mathcal{S}| \approx h^{-d}, \quad \min_{\mathcal{S}, \bar{\mathcal{S}}} |\mathcal{E}(\mathcal{S}, \bar{\mathcal{S}})| \approx h^{1-d}, \quad \text{and} \quad (\mathcal{L}v, v) \approx h^{2-d} |v|_{H^1(\Omega)}.$$

This matches the usual Poincaré inequality, because after rescaling  $(v, v) \approx h^{-d} \|v\|_{L^2(\Omega)}^2$  we have that  $(v, v) \lesssim (\mathcal{L}v, v) \approx |v|_{H^1(\Omega)}^2$  as expected.

## References

- [1] P. F. Antonietti, L. Beirão da Veiga, C. Lovadina, and M. Verani. Hierarchical a posteriori error estimators for the mimetic discretization of elliptic problems. *SIAM J. Numer. Anal.*, 51(1):654–675, 2013.
- [2] P. F. Antonietti, L. Beirão da Veiga, and M. Verani. Numerical performance of an adaptive MFD method for the obstacle problem. In *Numerical Mathematics and Advanced Applications. Proceedings of the 9th European Conference on Numerical Mathematics and Advanced Applications*, Springer Verlag Italia. Springer, Berlin, 2013.
- [3] P. F. Antonietti, L. Beirão da Veiga, N. Bigoni, and M. Verani. Mimetic finite differences for nonlinear and control problems. Technical Report MOX report 12/2013. Submitted for publication, 2012.
- [4] P. F. Antonietti, L. Beirão da Veiga, and M. Verani. A mimetic discretization of elliptic obstacle problems. *Math. Comp.*, 82(283):1379–1400, 2013.
- [5] P. F. Antonietti, N. Bigoni, and M. Verani. Mimetic finite difference approximation of quasilinear elliptic problems. Technical Report MOX-Preprint, 38/2012. Submitted for publication, 2012.
- [6] P. F. Antonietti, N. Bigoni, and M. Verani. Mimetic discretizations of elliptic control problems. *Journal of Scientific Computing*, 56(1):14–27, 2013.

- [7] L. Beirão da Veiga. A residual based error estimator for the mimetic finite difference method. *Numer. Math.*, 108(3):387–406, 2008.
- [8] L. Beirão da Veiga. A mimetic finite difference method for linear elasticity. *M2AN Math. Model. Numer. Anal.*, 44(2):231–250, 2010.
- [9] L. Beirão da Veiga, J. Droniou, and G. Manzini. A unified approach to handle convection terms in mixed and hybrid finite volumes and mimetic finite difference methods, 2011. To appear on IMA J. Numer Anal.; published online.
- [10] L. Beirão da Veiga, V. Gyrya, K. Lipnikov, and G. Manzini. Mimetic finite difference method for the Stokes problem on polygonal meshes. *J. Comput. Phys.*, 228(19):7215–7232, 2009.
- [11] L. Beirão da Veiga and K. Lipnikov. A mimetic discretization of the Stokes problem with selected edge bubbles. *SIAM J. Sci. Comp.*, 32(2):875–893, 2010.
- [12] L. Beirão da Veiga, K. Lipnikov, and G. Manzini. Convergence of the mimetic finite difference method for the Stokes problem on polyhedral meshes. *SIAM J. Numer. Anal.*, 48(4):1419–1443, 2010.
- [13] L. Beirão da Veiga, K. Lipnikov, and G. Manzini. Arbitrary-order nodal mimetic discretizations of elliptic problems on polygonal meshes. *SIAM J. Numer. Anal.*, 49:1737–1760, 2011.
- [14] L. Beirão da Veiga, K. Lipnikov, and G. Manzini. Arbitrary order nodal mimetic discretizations of elliptic problems on polygonal meshes. *SIAM J. Numer. Anal.*, 49:1737–1760, 2011.
- [15] L. Beirão da Veiga and G. Manzini. A higher-order formulation of the mimetic finite difference method. *SIAM J. Sci. Comp.*, 31(1):732–760, 2008.
- [16] L. Beirão da Veiga, F. Brezzi, A. Cangiani, G. Manzini, L. D. Marini, and A. Russo. Basic principles of virtual element methods. *Math. Models Methods Appl. Sci.*, 23(1):199–214, 2013.
- [17] L. Beirão da Veiga, F. Brezzi, and L. D. Marini. Virtual elements for linear elasticity problems. *SIAM J. Numer. Anal.*, 51(2):794–812, 2013.
- [18] L. Beirão da Veiga and D. Mora. A mimetic discretization of the Reissner–Mindlin plate bending problem. *Numer. Math.*, 117(3):425–462, 2011.
- [19] J. H. Bramble. *Multigrid methods*, volume 294 of *Pitman Research Notes in Mathematics Series*. Longman Scientific & Technical, Harlow, 1993.

- [20] F. Brezzi and A. Buffa. Innovative mimetic discretizations for electromagnetic problems. *J. Comput. Appl. Math.*, 234(6):1980–1987, 2010.
- [21] F. Brezzi, A. Buffa, and K. Lipnikov. Mimetic finite differences for elliptic problems. *M2AN Math. Model. Numer. Anal.*, 43(2):277–295, 2009.
- [22] F. Brezzi, A. Buffa, and K. Lipnikov. Mimetic finite differences for elliptic problems. *M2AN Math. Model. Numer. Anal.*, 43(2):277–295, 2009.
- [23] F. Brezzi, K. Lipnikov, and M. Shashkov. Convergence of the mimetic finite difference method for diffusion problems on polyhedral meshes. *SIAM J. Numer. Anal.*, 43(5):1872–1896, 2005.
- [24] F. Brezzi, K. Lipnikov, and M. Shashkov. Convergence of mimetic finite difference method for diffusion problems on polyhedral meshes with curved faces. *Math. Models Methods Appl. Sci.*, 16(2):275–297, 2006.
- [25] F. Brezzi, K. Lipnikov, M. Shashkov, and V. Simoncini. A new discretization methodology for diffusion problems on generalized polyhedral meshes. *Comput. Methods Appl. Mech. Engrg.*, 196(37-40):3682–3692, 2007.
- [26] F. Brezzi, K. Lipnikov, and V. Simoncini. A family of mimetic finite difference methods on polygonal and polyhedral meshes. *Math. Models Methods Appl. Sci.*, 15(10):1533–1551, 2005.
- [27] F. Brezzi and L. D. Marini. Virtual element methods for plate bending problems. *Comput. Methods Appl. Mech. Engrg.*, 253:455–462, 2013.
- [28] A. Cangiani and G. Manzini. Flux reconstruction and pressure post-processing in mimetic finite difference methods. *Comput. Methods Appl. Mech. Engrg.*, 197(9-12):933–945, 2008.
- [29] A. Cangiani, G. Manzini, and A. Russo. Convergence analysis of the mimetic finite difference method for elliptic problems. *SIAM J. Numer. Anal.*, 47(4):2612–2637, 2009.
- [30] B. Chazelle. Convex partitions of polyhedra: a lower bound and worst-case optimal algorithm. *SIAM J. Comput.*, 13(3):488–507, 1984.
- [31] J. Cheeger. A lower bound for the smallest eigenvalue of the Laplacian. In *Problems in Analysis*, pages 195–199. Princeton Univ. Press, 1970.
- [32] D. Cho, J. Xu, and L. Zikatanov. New estimates for the rate of convergence of the method of subspace corrections. *Numer. Math. Theory Methods Appl.*, 1(1):44–56, 2008.

- [33] J. Dodziuk. Difference equations, isoperimetric inequality and transience of certain random walks. *Transactions of the American Mathematical Society*, 284:787–794, 1984.
- [34] T. Dupont and R. Scott. Polynomial approximation of functions in Sobolev spaces. *Math. Comp.*, 34(150):441–463, 1980.
- [35] W. Hackbusch. *Multigrid methods and applications*, volume 4 of *Springer Series in Computational Mathematics*. Springer-Verlag, Berlin, 1985.
- [36] R. Hiptmair and J. Xu. Nodal auxiliary space preconditioning in  $\mathbf{H}(\mathbf{curl})$  and  $\mathbf{H}(\mathbf{div})$  spaces. *SIAM J. Numer. Anal.*, 45(6):2483–2509 (electronic), 2007.
- [37] X. Hu, S. Wu, X.-H. Wu, J. Xu, C.-S. Zhang, S. Zhang, and L. Zikatanov. Combined Preconditioning with Applications in Reservoir Simulation. *Multiscale Model. Simul.*, 11(2):507–521, 2013.
- [38] M. Jerrum and A. Sinclair. Approximating the permanent. *SIAM J. Computing*, 18:1149–1178, 1989.
- [39] J. K. Kraus. Algebraic multigrid based on computational molecules. II. Linear elasticity problems. *SIAM J. Sci. Comput.*, 30(1):505–524, 2007/08.
- [40] J. K. Kraus, P. S. Vassilevski, and L. T. Zikatanov. Polynomial of best uniform approximation to  $1/x$  and smoothing in two-level methods. *Computational Methods in Applied Mathematics*, 12(4):448–468, 2012.
- [41] I. Lashuk and P. S. Vassilevski. On some versions of the element agglomeration AMGe method. *Numer. Linear Algebra Appl.*, 15(7):595–620, 2008.
- [42] I. V. Lashuk and P. S. Vassilevski. Element agglomeration coarse Raviart-Thomas spaces with improved approximation properties. *Numer. Linear Algebra Appl.*, 19(2):414–426, 2012.
- [43] K. Lipnikov, G. Manzini, F. Brezzi, and A. Buffa. The mimetic finite difference method for the 3D magnetostatic field problems on polyhedral meshes. *J. Comput. Phys.*, 230(2):305–328, 2011.
- [44] K. Lipnikov, J. Moulton, and D. Svyatskiy. A Multilevel Multiscale Mimetic ( $M^3$ ) method for two-phase flows in porous media. *J. Comp. Phys.*, 227:6727–6753, 2008.
- [45] S. V. Nepomnyaschikh. Decomposition and fictitious domains methods for elliptic boundary value problems. In *Fifth International Symposium*

on *Domain Decomposition Methods for Partial Differential Equations* (Norfolk, VA, 1991), pages 62–72. SIAM, Philadelphia, PA, 1992.

- [46] J. E. Pasciak and P. S. Vassilevski. Exact de Rham sequences of spaces defined on macro-elements in two and three spatial dimensions. *SIAM J. Sci. Comput.*, 30(5):2427–2446, 2008.
- [47] P. S. Vassilevski. *Multilevel block factorization preconditioners*. Springer, New York, 2008. Matrix-based analysis and algorithms for solving finite element equations.
- [48] J. Xu. The auxiliary space method and optimal multigrid preconditioning techniques for unstructured grids. *Computing*, 56(3):215–235, 1996. International GAMM-Workshop on Multi-level Methods (Meis-dorf, 1994).
- [49] L. T. Zikatanov. Two-sided bounds on the convergence rate of two-level methods. *Numer. Linear Algebra Appl.*, 15(5):439–454, 2008.

# MOX Technical Reports, last issues

Dipartimento di Matematica “F. Brioschi”,  
Politecnico di Milano, Via Bonardi 9 - 20133 Milano (Italy)

- 50/2013** ANTONIETTI, P.F.; VERANI, M.; ZIKATANOV, L.  
*A two-level method for Mimetic Finite Difference discretizations of elliptic problems*
- 49/2013** MICHELETTI, S.  
*Fast simulations in Matlab for Scientific Computing*
- 48/2013** SIMONE PALAMARA, CHRISTIAN VERGARA, ELENA FAGGIANO, FABIO NOBILE  
*An effective algorithm for the generation of patient-specific Purkinje networks in computational electrocardiology*
- 47/2013** CHKIFA, A.; COHEN, A.; MIGLIORATI, G.; NOBILE, F.; TEMPONE, R.  
*Discrete least squares polynomial approximation with random evaluations - application to parametric and stochastic elliptic PDEs*
- 46/2013** MARRON, J.S.; RAMSAY, J.O.; SANGALLI, L.M.; SRIVASTAVA, A.  
*Statistics of Time Warpings and Phase Variations*
- 45/2013** SANGALLI, L.M.; SECCHI, P.; VANTINI, S.  
*Analysis of AneuRisk65 data: K-mean Alignment*
- 44/2013** SANGALLI, L.M.; SECCHI, P.; VANTINI, S.  
*AneuRisk65: a dataset of three-dimensional cerebral vascular geometries*
- 43/2013** PATRIARCA, M.; SANGALLI, L.M.; SECCHI, P.; VANTINI, S.  
*Analysis of Spike Train Data: an Application of K-mean Alignment*
- 42/2013** BERNARDI, M.; SANGALLI, L.M.; SECCHI, P.; VANTINI, S.  
*Analysis of Juggling Data: an Application of K-mean Alignment*
- 41/2013** BERNARDI, M.; SANGALLI, L.M.; SECCHI, P.; VANTINI, S.  
*Analysis of Proteomics data: Block K-mean Alignment*